

Transverse tensile properties of an unbonded model composite

B. R. BUTCHER

Metallurgy Division, UKAEA Research Group, AERE, Harwell, UK

Models of unbonded composites have been made by drilling holes in aluminium alloy strip and plugging the holes with steel rods. These specimens, together with similar specimens left unplugged, have been tested in tension. Young's modulus, stress at the elastic limit and ultimate tensile stress have been measured. The results, particularly for the Young's modulus of the plugged strips, show a complex behaviour. The application of the results to real materials is discussed.

1. Introduction

There is a small number of cermet composites which are characterized by having no chemical bond between the included phase and the matrix. Chief among them are nuclear fuel cermets of the type in which UO_2 spheroids are embedded in a metallic matrix, and carbon fibre composites with such metals as lead and tin. In the latter composites with unidirectional fibres, there appears to be a mechanical keying of the matrix to the fibres such that a substantial proportion of the potential tensile strength parallel to the fibre direction can be realized [1]. Little is known of the tensile strength perpendicular to the fibre direction, but it seems that in this direction the key is poor, or entirely lacking [1].

With the former materials, one can read in the literature that a certain manufacturing route leads to good mechanical properties. This statement only has meaning if it signifies that the properties are better than those resulting from another manufacturing route, as the optimum mechanical properties of such materials are unknown. There is no adequate theory: simple theories [2, 3] of tensile strength are based on the calculated minimum cross sectional area of a cermet, and do not take into account packing variations, while more complex theories [4, 5] make use of stress concentration effects of doubtful validity.

Lacking a theory, ideally one would like to take both of these materials, and eliminating such experimental variables as porosity and inclusion content, vary the packing in a system-

atic manner. The experimental difficulties would be formidable. Failing a suitable real material, a model system might be used.

It is the purpose of this paper to describe work on such a model. Steel plugs were force fitted into various patterns of holes drilled in an aluminium alloy strip, and the tensile properties of this composite were studied. It is believed that the results have a direct qualitative analogy with the transverse properties of carbon fibres in metals, and relevance to the properties of the nuclear fuel cermets.

2. Experimental materials and method

The "matrix" material was 10 SWG (3.25 mm thick) sheet of aluminium-2 $\frac{1}{4}$ % magnesium alloy. Two basic patterns of holes were used (Fig. 1), the square (or S) pattern, and the diamond (or D) pattern. The three variables imposed were:

(a) Volume fraction. The distance between lines of holes (a , Fig. 1) was made equal to the distance between rows of holes (b , Fig. 1), and the volume fraction was varied by increasing the radius of the holes. This simple arrangement was varied by increasing the radius of the holes. This simple arrangement was adopted rather than the complex one of keeping the hole size constant and varying " a " and " b ", as there is evidence that the size of the included ceramic, within certain limits, has no effect on the strength [6]. The volume fraction is signified by placing an integer after the S or D equal to ten times the nominal volume fraction: e.g. D3 stands for a specimen of diamond pattern containing a

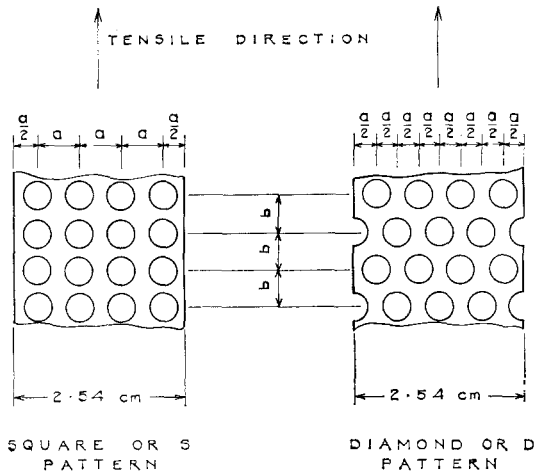


Figure 1 Basic patterns of specimen.

nominal volume fraction of included phase of 0.3.

(b) The ratio of “*a*” and “*b*” was varied in specimens D4 and S4. “*a*” was kept constant, so to keep the volume fraction approximately constant the radius of the holes had to be varied.

(c) To obtain some idea of the effect of random variations in packing and particle spacing that occur in the real materials, with the S1, D1, S2 and D2 specimens, the centres of the holes were moved parallel or perpendicular to the tensile direction in both “positive” and “negative” directions by amounts proportional to the digits taken from a table of random numbers, with the proviso that the holes should not overlap.

Half the specimens were left unplugged; these served as a standard of comparison (O specimens). The other half had the holes plugged with ground silver steel rods (P specimens). The machining specification was such that the plugs were between approximately 12 and 40 μm larger in diameter than the holes. All specimens were annealed at 300°C and air cooled. This treatment led to full recrystallization of the half-hard sheet. Two nominally identical specimens were tested for each result.

All specimens were tensile tested in a Mayes Universal Testing Machine. For measurement of Young’s modulus, the specimens were step-loaded, and small strains were measured over a 10 cm length with a Mayes dual extensometer. The accuracy of measurement of Young’s modulus was about 2%. For yield and UTS measurements, the crosshead speed was 1.5 mm/

min. The gauge length was approximately 10 cm, depending on the type of specimen.

Summary of nomenclature: S = square pattern of holes, D = diamond pattern of holes, O = open holes, P = plugged holes, number is 10 times the approximate volume fraction.

3. Results

3.1. The effect of volume fraction

3.1.1. Elastic properties

Fig. 2 shows the Young’s moduli of the unplugged specimens. Each point is the average of two results, the greatest difference between two nominally identical specimens being about 4% of the modulus.

Fig. 3 shows tensile loading and unloading curves for one of the S2P specimens. These show:

- (i) The slope of the initial loading curve I is always less than the slope of the repeat loading curve II at the same load. Thus the initial application of a load, however small, leads to a small permanent set in the specimen when the load is removed.
- (ii) Providing time is allowed for transient creep to diminish to zero at the maximum load attained, the specimens can then be cycled elastically to this load.
- (iii) In the elastic cycle, the modulus decreases with increasing elastic strain.
- (iv) In the elastic cycle, there is a small hysteresis between the loading and unloading curves. This is a genuine effect, as it did not occur with the O specimens.
- (v) The modulus at a given load decreases with increasing amounts of plastic strain in a previous strain cycle. This is illustrated in Fig. 4.

At about 0.1% plastic strain, the hysteresis had almost disappeared (curve IX, Fig. 3). The moduli at low load and 4.5 kN were respectively $4.52 \times 10^3 \text{ kN cm}^{-2}$ and $4.31 \times 10^3 \text{ kN cm}^{-2}$, and the modulus on unloading was constant at $4.37 \times 10^3 \text{ kN cm}^{-2}$. These values compare with an average modulus for the S20 specimens of $4.38 \times 10^3 \text{ kN cm}^{-2}$. Thus after about 0.1% plastic strain, the modulus of the plugged specimen has reverted to the modulus of a similar unplugged specimen.

Similar results were obtained with one specimen D4P, and the behaviour would seem characteristic of the P specimens.

With such complex behaviour, there is some difficulty in selecting and presenting the data for the P specimens. The method finally chosen was

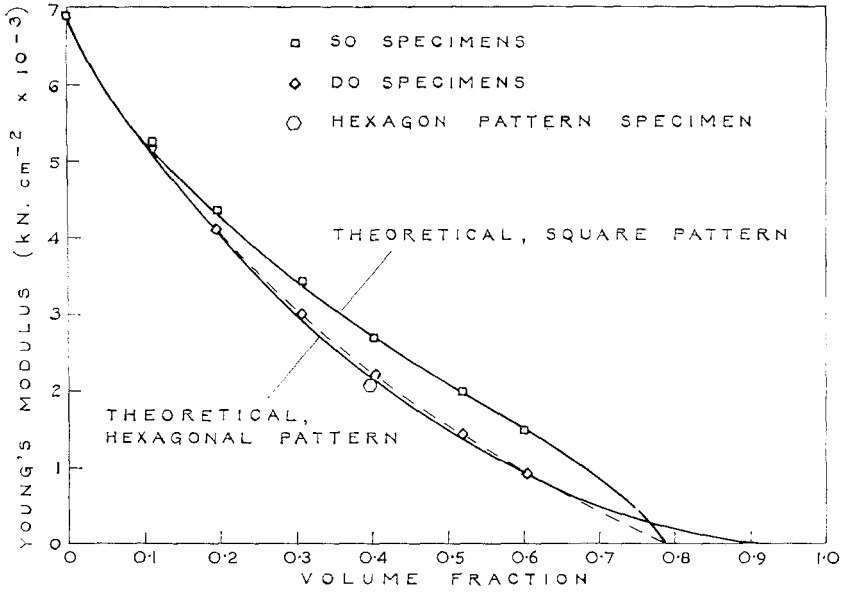


Figure 2 Young's modulus as a function of volume fraction for the unplugged specimens.

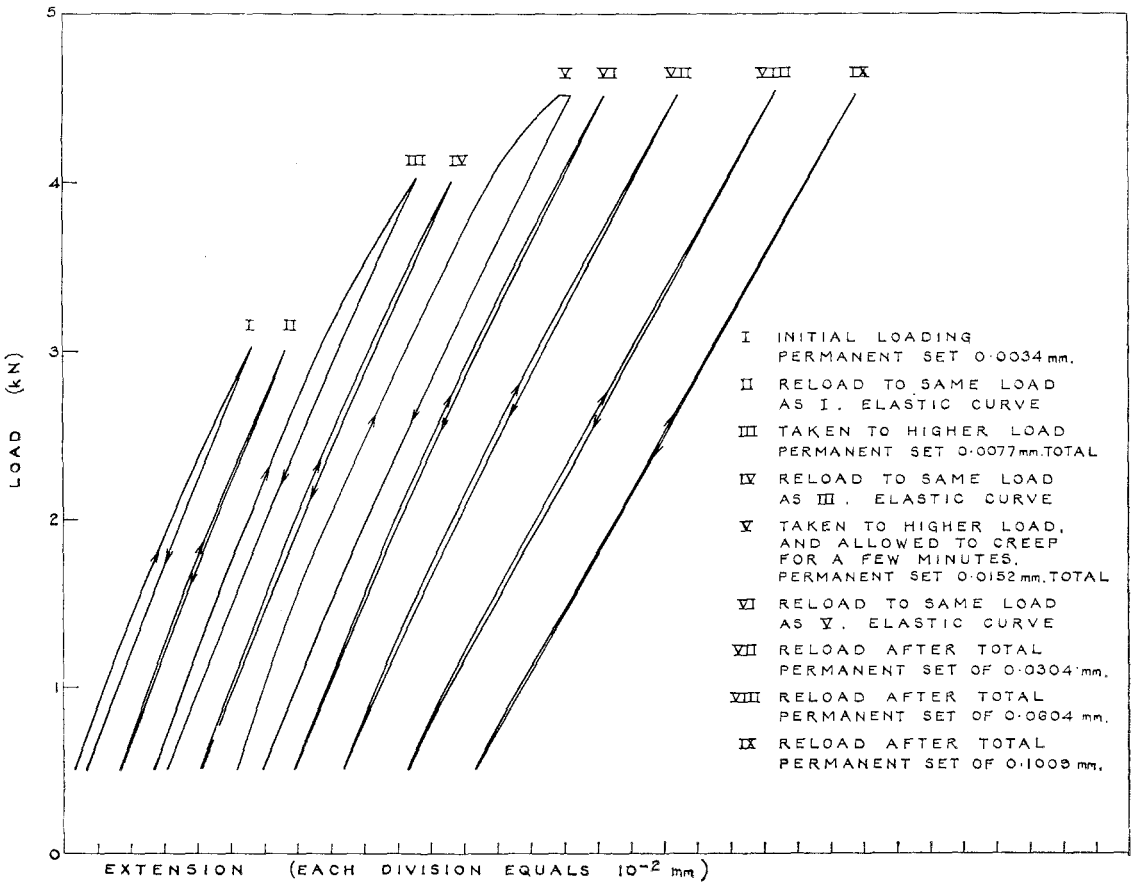


Figure 3 Load/extension curves for a plugged specimen, S2P.

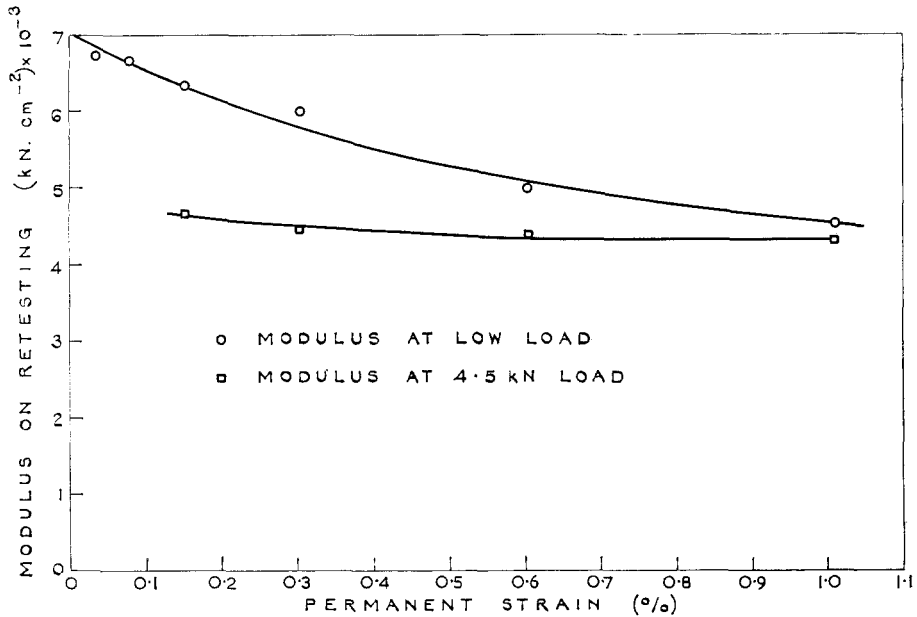


Figure 4 Young's modulus as a function of plastic strain for a plugged specimen.

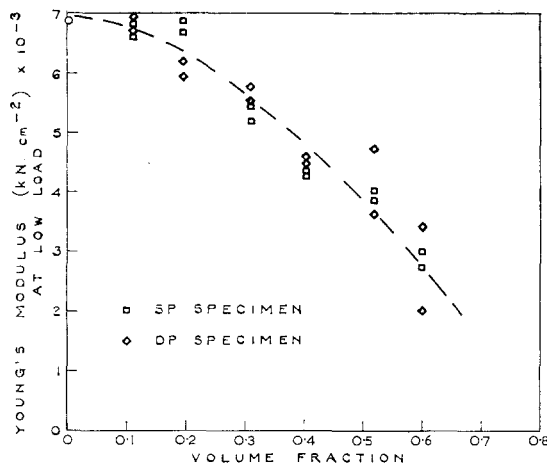


Figure 5 Young's modulus as a function of volume fraction, plugged specimens.

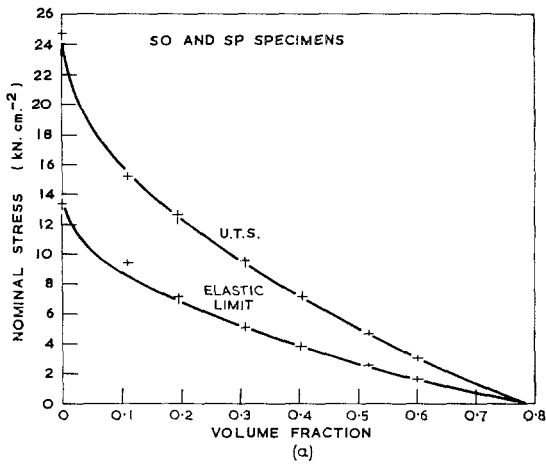
to measure the modulus at a low load, after an initial small permanent set. This low load was about one fifth of the load at the elastic limit* of a similar unplugged specimen, and the small permanent set always represented less than 0.01% plastic strain. For example, in Fig. 3, the modulus chosen for presentation was that between the loads 1.0 and 1.5 kN in curve II, as the load at the elastic limit of the S20 specimen was

*See later for definition of "elastic limit".

5.8 kN This gave a method of comparing the moduli of specimens with different volume fractions, shown in Fig. 5. There are large variations between nominally identical specimens, so careful extrapolation of the data to zero load and zero plastic strain to give the maximum modulus for each specimen is not justified. Data about moduli at higher loads is not presented, as the minimum modulus for any specimen after a small plastic strain has been induced in it, is obviously the modulus of a similar unplugged specimen.

3.1.2. Plastic behaviour

There was very little difference in the plastic flow of the plugged and unplugged specimens of identical pattern. Strengths of each type of pattern are given in Figs. 6a and b. The load at 0.002% plastic strain was also measured for the O specimens; this was in an attempt to see if the yield was affected by the stress concentration effect of the holes. The results were erratic, however, presumably due to slight straightening of the specimens. Thus the load at the elastic limit, measured by the first observable departure from straight line behaviour in the record of the load-time chart recorder, was used as a measure of proof stress. This measurement was also applied to the P specimens, and worked success-



LENGTH OF LINE MARKS RANGE OF RESULTS, CROSS GIVES AVERAGE RESULT.

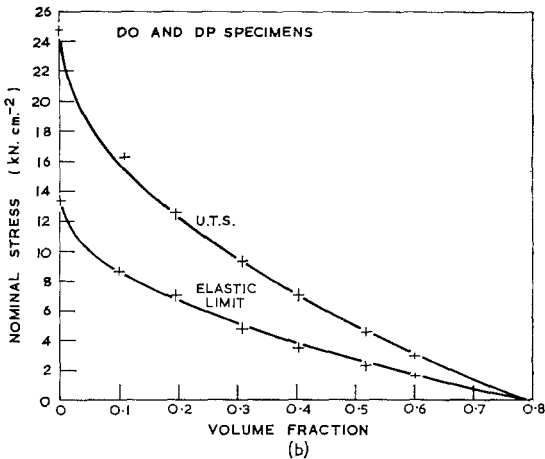


Figure 6 Strength of specimens as a function of volume fraction.

fully because of the greatly reduced strain sensitivity in the recording method used. The elastic limit of one each of the S2P and D4P specimens could be compared directly with the results from nominally identical specimens, where the stress was measured for small plastic strains (in the course of producing Fig. 3 for S2P, for example). This comparison suggested that the plastic strain at the "elastic limit" was approximately 0.05%. Figs. 6a and b are almost identical.

Strain to fracture was also measured, and is shown in Figs. 7a and b. These, too, are almost identical except at low volume fractions.

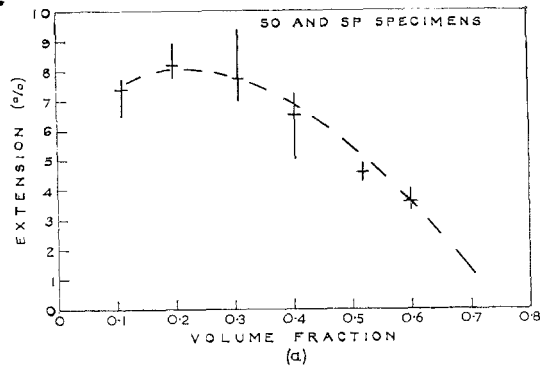
Deformation at higher volume fractions occurred solely in the "vertical" webs, i.e. in those webs whose plane of symmetry contained

the tensile axis. Since there was no deformation elsewhere, there was virtually no overall reduction of area. This was also true of the lower volume fractions, as deformation in the majority of the matrix was small compared to that in the vertical webs. All but three specimens broke by the webs in a single row fracturing almost simultaneously; the thin webs at the end of a row were the first to break in both S and D patterns. In the three exceptions, one thicker vertical web broke well in advance of the others in the same row, and this led to a low UTS and low strain to fracture. These results are not included in Figs. 6 and 7.

Necking took place only in those webs that fractured. Nevertheless all the pegs were loose in their holes in the broken specimens, because of the reduction of area of each vertical web caused by its plastic extension.

3.2. The effect of the ratio of row spacing to line spacing

The properties of specimens with varying b/a



LENGTH OF LINE MARKS RANGE OF RESULTS, CROSS GIVES AVERAGE RESULT.

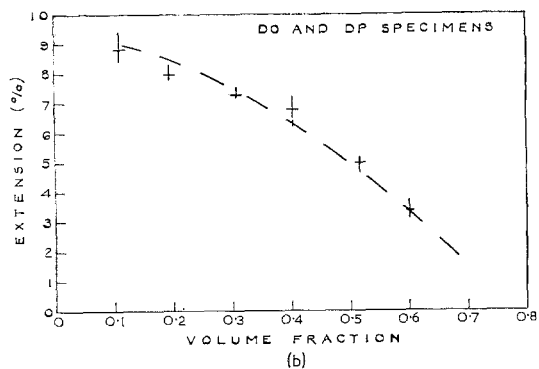


Figure 7 Extension of specimens as a function of volume fraction.

TABLE I Properties of specimens containing a nominal volume fraction of 0.4 of the second phase

<i>b/a</i> ratio	Volume Fraction	Hole diameter (mm)	Type	Young's Modulus <i>E</i> (10 ⁸ kN cm ⁻²)	<i>E</i> at low load (10 ⁸ kN cm ⁻²)	Nominal stress at elastic limit (kN cm ⁻²)	Nominal UTS (kN cm ⁻²)	Stress at elastic limit in min. area (kN cm ⁻²)	UTS in min. area (kN cm ⁻²)	Extension %	Comments
1.0	0.403	4.55	S40	2.66	—	3.9	7.2	13.9	25.4	7.4	Square pattern for S specimens
			D40	2.19	—	3.6	7.1	12.8	25.1	7.3	
			S4P	—	4.25	3.7	7.0	13.0	24.8	7.4	
0.866	0.400	4.20	D4P	—	4.33	—	—	—	—	—	Hexagonal pattern for D specimens
			D4P	—	4.49	3.3	6.8	12.0	23.9	7.1	
			D4P	—	4.51	—	—	—	—	—	
0.592	0.404	3.50	S40	2.94	—	5.5	8.4	16.5	25.0	5.6	Minimum thickness of diagonal webs
			D40	2.11	—	5.1	8.1	15.1	24.1	6.7	
			S4P	—	5.09	5.4	8.1	16.1	24.0	5.0	
0.592	0.404	3.50	D4P	—	4.25	—	—	—	—	—	half minimum thickness of vertical webs, D pattern
			D4P	—	4.93	5.2	8.1	15.6	24.3	5.8	
			D4P	—	5.03	—	—	—	—	—	
0.592	0.404	3.50	S40	3.52	—	6.9	11.0	15.4	24.7	9.8	Minimum thickness of diagonal webs
			D40	1.53	—	3.8	8.3	8.5	18.5	24.4*	
			S4P	—	6.53	6.8	10.9	15.2	24.5	9.5	
0.592	0.404	3.50	D4P	—	7.04	—	—	—	—	—	half minimum thickness of vertical webs, D pattern
			D4P	—	8.07	4.9	8.7	10.9	19.4	12.5*	
0.592	0.404	3.50	D4P	—	7.86	—	—	—	—	—	half minimum thickness of vertical webs, D pattern
			D4P	—	—	—	—	—	—	—	

*Uniform extension. All other results in this column, total extension.

ratio are given in Table I. As before, average values are given except for the modulus at low load of the P specimens, where individual results are shown. For the O specimens, Young's modulus increases with decreasing *b/a* ratio for the S pattern and decreases with the D pattern. The result for the hexagonal pattern is plotted in Fig. 2. For the P specimens, however, the modulus at low load increases with decreasing *b/a* ratio for both patterns, although there are still some large differences between nominally identical specimens.

As well as the nominal yield and UTS, the yield and UTS in the minimum cross section are listed. These are defined as the nominal stress multiplied by the ratio of nominal area to the minimum cross-sectional area. The plastic properties of specimens D40 and D4P with a *b/a* ratio of 0.592 should be noted both in relation to each other and to the other specimens. Deformation in these specimens was by shear in the diagonal webs, i.e. in those webs whose plane of symmetry lay at an acute angle to the tensile axis. The shear was very large in the D4O

specimens, leading to the collapse of the holes. This collapse was prevented by the plugs in the D4P specimens restricting the shear (Fig. 8). Measurement of web thicknesses showed that there had been no deformation in the vertical webs. Fracture in these specimens was, of course, by shear of the diagonal webs.

3.3. The effect of the "random" placing of holes

Table II gives the properties of the specimens of nominally the same volume fraction, but with regular or random arrays. At the lower volume fraction, the main effect of the random nature of the holes or plugs is on the UTS, but at the higher volume fraction, every property except, apparently, *E* at low load, is decreased in the random specimens.

Breaking of the random specimens was a drawn-out process, with a thin web fracturing first, followed sometime later by another web, and so on until the fracture was across the whole specimen. Shear fracture of a web took place in both S and D type specimens.

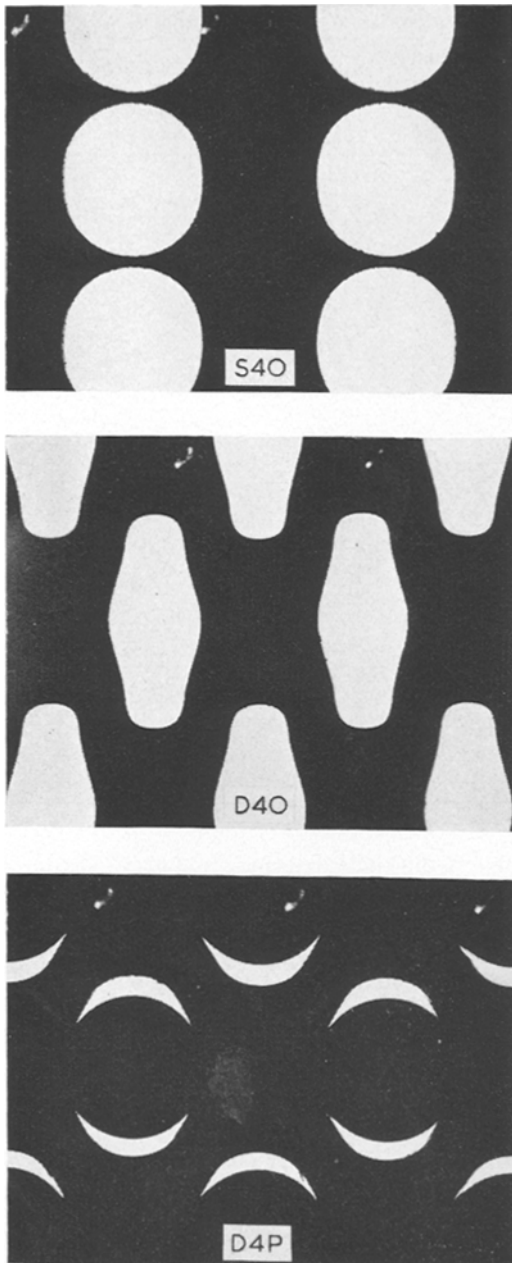


Figure 8 Hole shape and web thickness in broken specimens with $b/a = 0.592 (\times 5)$.

4. Discussion

4.1. Results

4.1.1. Elastic properties

The continuous lines in Fig. 2 were drawn using the theoretical results for the moduli given by Grigolyuk and Fil'shtinskii [7]. The upper one

refers to a square pattern of holes in plate, and the lower to a hexagonal pattern. The results for the SO specimens lie very close to the theoretical line, showing that the edge effect in these specimens, due to the small number of holes in the rows perpendicular to the tensile axis, had only a small influence. The single result for a hexagonal pattern also lies close to the theoretical line. The results for the DO specimens (dashed line) are self consistent and lie, as expected, between the two sets of theoretical values, thus the edge effect in these was also probably small. The reason for the decrease in E in the random patterns of the S20 and D20 specimens (Table II) is not clear, but might be connected with increased stress concentration in the random arrays.

The plugged specimens were annealed at 300°C , and it can be assumed that the stresses developed when the plugs were forced into the holes diminished almost to zero at the annealing temperature. On cooling, however, as the thermal expansion coefficient of the aluminium alloy is about twice that of the steel, stresses would develop locally around the plugs, which in the aluminium matrix at room temperature would exceed its yield stress. Thus any applied stress, however small, would lead to further local plastic strain, and a permanent set on unloading. If the contact between the steel and the aluminium were perfect it might be expected: (i) that the properties of nominally identical specimens should be almost identical, as with the unplugged specimens, (ii) that the Young's modulus at low load, measured as described herein, might approach that of a similar bonded material, as the small strains set up by the applied load in the matrix adjacent to a plug would not entirely relieve the radial compressive stress in the plug in any direction.

The method of manufacturing the specimens was such that perfect contact between plug and matrix was impossible to achieve. Difference in contact area is the only uncontrolled variable that could account for the difference between nominally identical specimens. It is reasonable to suppose that the less the initial contact area, the lower the modulus. Thus the decrease in modulus with both increasing elastic and plastic strain can be accounted for by decrease in contact area as a result of elastic or plastic strains. At about 0.1% plastic strain, the modulus reverted to that of the unplugged material, so presumably that was the stage where

TABLE II Properties of specimens containing nominal volume fractions 0.1 and 0.2 second phase

Type	Array	E (10^3 kN cm $^{-2}$)	E at low load (10^3 kN cm $^{-2}$)	Nominal stress at elastic limit (kN cm $^{-2}$)	Nominal UTS (kN cm $^{-2}$)	Stress at elastic limit in min. area (kN cm $^{-2}$)	UTS in min. area (kN cm $^{-2}$)	Total Extension (%)
S1O	regular	5.24	—	9.4	15.2	15.1	24.4	7.3
D1O	regular	5.21	—	8.6	16.2	13.8	25.9	8.9
S1O	random	5.21	—	7.8	13.9	12.5	22.3	7.4
D1O	random	5.10	—	9.0	12.3	14.4	19.6	3.8
S1P	regular	—	6.66 6.81	9.4	15.1	15.1	24.2	7.1
D1P	regular	—	6.92 6.68	8.7	16.2	13.9	25.9	8.6
S1P	random	—	6.74 6.90	7.4	13.7	11.8	21.0	7.7
D1P	random	—	6.45 6.58	8.5	12.1	13.6	19.4	4.1
S2O	regular	4.38	—	7.0	12.8	14.0	25.6	8.6
D2O	regular	4.12	—	7.0	12.4	14.0	24.8	8.1
S2O	random	3.86	—	6.3	9.5	12.6	19.0	6.2
D2O	random	3.71	—	6.5	8.5	13.0	17.0	5.6
S2P	regular	—	6.69 6.87	7.2	12.4	14.4	24.8	7.8
D2P	regular	—	5.96 6.20	7.3	12.8	14.6	25.6	7.8
S2P	random	—	6.25 6.71	6.0	9.7	12.0	19.5	5.9
D2P	random	—	5.78 5.57	6.4	8.7	12.8	17.4	3.8

there was only fragmentary line contact on the plug in a plane perpendicular to the tensile axis. Moreover, the discrepancy between the measured modulus and the theoretical modulus for a similar bonded material increased as the volume fraction increased. This could be due to the fractional area of contact decreasing with increasing diameter of the plug. The machining tolerance was constant, so that the fraction of plastic accommodation of the misfit to the elastic accommodation would decrease with increasing plug diameter.

The small hysteresis in the loading and unloading curves of these specimens was presumably due to friction between plug and matrix.

These results from the plugged specimens are at variance with those of Chen and Lin [8], who found that the transverse modulus followed a law of mixtures whether the composite was bonded or unbonded. Their method of measuring the modulus was not stated.

4.1.2. Plastic properties

The lines connecting the points in Fig. 6 were

drawn from the equation

$$\sigma_v = \sigma \left(1 - 2 \sqrt{\frac{V}{\pi}} \right) \quad (1)$$

where σ_v is the nominal stress in the minimum cross sectional area of a specimen containing a volume fraction V of inclusion, σ is either the UTS or the stress at the elastic limit of a standard test piece of the aluminium alloy sheet, and, when a equals b ,

$$1 - 2 \sqrt{\frac{V}{\pi}} = \frac{a - 2r}{a}$$

= minimum fractional cross section. So calculations of strength from the minimal cross sectional area are valid in regular packing when $a = b$. Both the stress at the elastic limit, measured macroscopically, and the UTS are accounted for by this concept, without introducing stress concentration factors. It also accounts for the results when $b/a < 1$, providing the true minimum area is used, until shear at the diagonal webs occurs. (See Table I. The small discrepancy in proof stress between specimens with $b/a = 1$ and $b/a = 0.866$ in Table I is not regarded as

serious as the former were annealed at a different time and may have received a slightly different treatment.) If the simple formula (Equation 1) was used however, the stress in the minimum area would be over estimated. When the deformation occurs by shear (specimens D4O and D4P with $b/a = 0.592$, Table I) the minimum area concept does not work because it is entirely irrelevant to the process involved. The nominal UTS of these specimens is, however, about the same as that of the specimens with a b/a ratio of 0.866.

A low UTS of webs with varying minimum thickness can be explained when the webs are acting in parallel (Appendix I), if the extension of an individual web decreases with decreasing minimum dimension, as it seems to (Fig. 7 and see later). However, in pure aluminium, when the holes in a single row were staggered in a direction parallel to the tensile direction, the nominal UTS was greater than that of a row of holes with their centres on a line perpendicular to the tensile direction [9]. It seems that in the present specimens the effect of varying web thickness outweighs the effect of staggering the holes, tending to a low UTS (Table II).

Strictly speaking, the argument in Appendix I can also be applied to the thin outer webs in the specimens with regular arrays. However, as already noted all webs in these specimens broke almost simultaneously. Thus the extension of the outer webs must have been almost equal to the extension of the thicker inner webs: this might be ascribed to the outer webs being bounded on one side by a plane surface. This coincidence of extensions led to the confirmation of the simple minimum area law for the UTS (Equation 1).

The simple model in Appendix I does not explain the low stress at the elastic limit in the specimens with random arrays. For the D patterns it may have been that the true minimum cross section projected in the tensile direction was less than the assumed minimum cross section. This could not have been true for the S specimens. Fig. 9 does show, however, that for a given extension the load is always lower for the webs of varied dimension. Thus the load at which the departure from elasticity was noticed, i.e. at which a given small strain could be detected, may have been lower for the random arrays.

At high volume fractions, where deformation was only in the vertical webs, the total extension rose with decreasing volume fraction, or increasing minimum dimension of web, thus justifying to

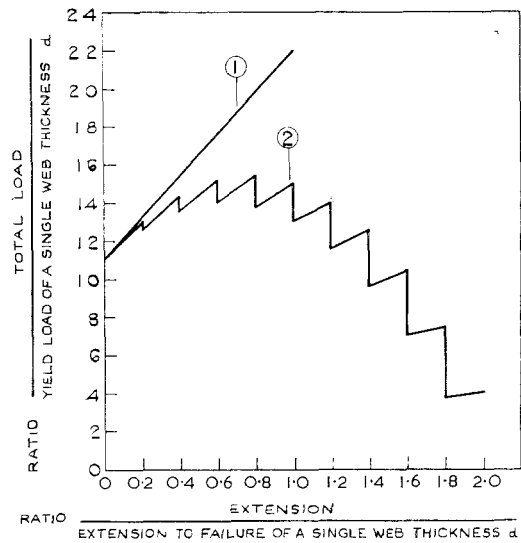


Figure 9 Load/extension curves for uniform and varying webs.

- ① 11 Webs of equal minimum size d .
- ② 11 Webs of size varying equally from 0 to $2.0 d$.

some extent the assumption in Appendix I. But at the lowest volume fractions, the minimum web thickness was comparable to the thickness of the plate. Thus the extension for the S specimens was roughly constant at low volume fraction (Fig. 7a). In the D specimens, the continuing increase in extension with decreasing volume fraction might be attributed to a small amount of shear in the diagonal webs. The results on extension are included mainly to show the remarkable differences engendered by shear in the diagonal webs of the D4 specimens, and are not considered greatly relevant to the properties of real materials.

4.2. Application to real materials

Micrographs of carbon fibre composites (Fig. 10) suggest that at high volume fraction, the packing can be regarded as a series of distorted hexagons. For cermet fuels, manufacturing by pressing methods would not produce alignment of spherical inclusions. Thus discussion will make use of the results on the DP specimens only. Most methods of making the real materials involve consolidation at high temperature, followed by cooling. The stresses in the real materials will be similar in pattern to those in the model. Thus the real cermets will take up a small permanent set when a load is applied, and

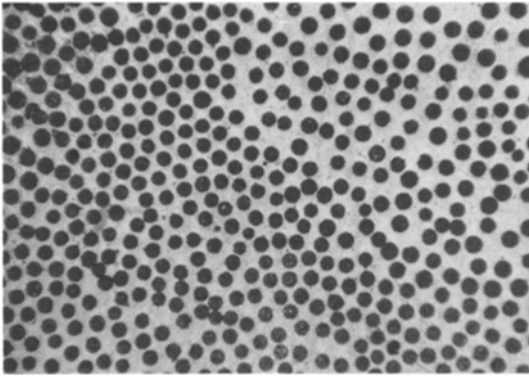


Figure 10 Carbon fibres in tin ($\times 260$). (Courtesy of D. C. Minty).

the modulus will vary with elastic and plastic strain. However, the modulus at low load will depend on the intimacy of contact between the included phase and the matrix; i.e. it will depend on the manufacturing method, and if nearly perfect contact is achieved, the modulus could approach that of a similar bonded specimen. It is also probable that hysteresis would occur between loading and unloading, and in situations where the stress cycles rapidly, self-heating effects might take place in the materials.

Since some irregular packings lead to low strengths, it will pay to give some attention to uniform spacings between particles during manufacture. Isostatic pressing methods would produce uniform strength perpendicular to the fibre direction in fibre composites, and isotropic strength in the other type. This strength would be a little below that predicted by simple theories [2, 3] because of irregularities in the packing, although in the carbon fibre composite, the strength of the matrix in the webs would be higher than its strength in bulk because of the restriction of dislocation flow in webs of less than $1\ \mu\text{m}$ minimum thickness. However, in some cases it might be advantageous to use unidirectional pressing, as this would give high strengths in the pressing direction. Increasing displacements in the pressing direction during unidirectional pressing would continue to increase the UTS in this direction, but might lower the yield stress because of shear in diagonal webs.

The cermets would be far more susceptible to dirt and porosity in the matrix than the matrix material alone, because the dirt or porosity in the deforming webs would reduce their extension to failure, thus prematurely throwing the load onto the remaining webs, leading to low strength.

5. Summary of results and conclusions on "cermets"

The main technological interest in this work arises because the plugged specimens represent unbonded composites. In the following paragraphs the results and conclusions from these specimens, which might well apply to real materials, are summarized. The work on the specimens with unfilled holes is not summarized for the sake of brevity.

- (1) The Young's modulus at low strain of the cermet materials depends mainly on the volume fraction of included phase, and the area of contact between the included phase and the matrix. Packing variations are less important.
- (2) The Young's modulus decreases with increasing amounts of elastic and plastic strain. After a small plastic strain Young's modulus decreases to that of a "porous" material of the same volume fraction.
- (3) The initial application of a load produces a small permanent set in the cermet material.
- (4) There is a small hysteresis between elastic loading and unloading.
- (5) The strength of the material depends on the packing. It increases with decreasing b/a ratio, where b is the distance between included phase particles parallel to the tensile direction, and a is the corresponding distance perpendicular to the tensile direction. It decreases with increasing non-uniformity of packing.
- (6) Factors affecting the strength can be explained qualitatively without recourse to stress concentration factors, although these may play some part.
- (7) The manufacturing process could strongly affect the packing and contact between the matrix and included phase, in turn affecting the strength and Young's modulus of the material. Inclusion and porosity content in the matrix material will also strongly affect the strength.

Appendix I

The effect of varying web size on the UTS

The effect is perhaps best illustrated by a numerical example. Assume, for a web of minimum dimension d , a linear load/extension curve

$$P = P_0 + \epsilon \left(\frac{P_u - P_0}{\epsilon_u} \right)$$

where P is the load, ϵ is the extension, P_0 is the yield load, P_u is the breaking load, and ϵ_u is the extension to failure. If there are 11 such webs

acting in parallel, the load on these will be 11 times the load on a single web.

Take another 11 webs acting in parallel at minimum dimensions $0, 0.2d, 0.4d, \dots, 1.8d, 2.0d$. Total thickness = $11d$.

Assume that the extension to failure is proportional to the minimum dimension. It is known that the stress on the webs is constant; thus the load is also proportional to the minimum dimension. The load extension curves will be

$$P_2 = 0.2P_0 + \epsilon \left(\frac{P_u - P_0}{\epsilon_u} \right)$$

$$P_3 = 0.4P_0 + \epsilon \left(\frac{P_u - P_0}{\epsilon_u} \right)$$

etc, where P_2 is the load on the web of dimension $0.2d$, and P_3 is the load on the web of dimension $0.4d$, etc. Thus the total load up to extension $0.2 \epsilon_u$,

$$P_t = 11P_0 + 10 \frac{\epsilon}{\epsilon_u} (P_u - P_0)$$

At this extension, a web will break, and if the testing machine is perfectly hard, the load will drop, and the total load will become

$$P_t = 10.8 P_0 + 9 \frac{\epsilon}{\epsilon_u} (P_u - P_0)$$

up to an extension $0.4 \epsilon_u$, when another web will break, and so on.

If a reasonable ratio of P_u to P_0 is postulated, the normalized load/extension graph for each system can be drawn. The result for $P_u/P_0 = 2$ is shown in Fig. 9. In this case, the maximum

load on the non-uniform webs is 70% of the breaking load of the uniform webs.

Other more elaborate equations for load/extension may be adopted [9], but as long as the extension to failure of a web decreases with decreasing minimum dimension of the web, the principle remains.

Acknowledgements

The author would like to thank Mr D. C. Minty for permission to use Fig. 10, and for his help, together with that of Mr H. R. Strong, in the very early stages of this work. He would also like to thank Mr S. F. Pugh for his usefully discursive interest.

References

1. B. W. HOWLETT, D. C. MINTY, and C. F. OLD, "Int. Conf. on Carbon Fibres, Their Composites and Applications" (Plastics Inst, London, 1971), to be published.
2. M. EUDIER, *Powder Metall.* No. 9 (1962) 278.
3. B. R. BUTCHER and B. W. HOWLETT, *Int. J. Powder Met.* 2 (4) (1966) 29.
4. G. D. MCADAM, *Powder Metall.* 10 (20) (1967) 307.
5. R. HAYNES, *Powder Metall.* 14 (27) (1971) 64.
6. L. H. COPE, *Metallurgia*, 72 (1965) 165.
7. E. I. GRIGOLYUK and L. A. FIL'SHTINSKII "Perforated Plates and Holes" (Nauka, Moscow, 1970).
8. P. E. CHEN and J. M. LIN, *Mats. Res. and Stand.* 9 (1969) 29.
9. B. R. BUTCHER, *Eng. Fracture Mech.* 3 (1971) 191.

Received 17 December 1971 and accepted 11 February 1972.